Biophys Rev (2017) 9:669–682
DOI 10.1007/s12551-017-0296-0

REVIEW

Lipid-packing perturbation of model membranes by pH-responsive antimicrobial peptides

Dayane S. Alvares[1] · **Taisa Giordano Viegas**[1] · **João Ruggiero Neto**[1]

Received: 25 May 2017 / Accepted: 27 July 2017 / Published online: 29 August 2017

Abstract The indiscriminate use of conventional antibiotics is leading to an increase in the number of resistant bacterial strains, motivating the search for new compounds to overcome this challenging problem. Antimicrobial peptides, acting only in the lipid phase of membranes without requiring specific membrane receptors as do conventional antibiotics, have shown great potential as possible substituents of these drugs. These peptides are in general rich in basic and hydrophobic residues forming an amphipathic structure when in contact with membranes. The outer leaflet of the prokaryotic cell membrane is rich in anionic lipids, while the surface of the eukaryotic cell is zwitterionic. Due to their positive net charge, many of these peptides are selective to the prokaryotic membrane. Notwithstanding this preference for anionic membranes, some of them can also act on neutral ones, hampering their therapeutic use. In addition to the electrostatic interaction driving peptide adsorption by the membrane, the ability of the peptide to perturb lipid packing is of paramount importance in their capacity to induce cell lysis, which is strongly dependent on electrostatic and hydrophobic interactions. In the present research, we revised the adsorption of antimicrobial peptides by model membranes as well as the perturbation that they induce in lipid packing. In particular, we focused on some peptides that have simultaneously acidic and basic residues. The net charges of these peptides are modulated by pH changes and the lipid composition of model membranes. We discuss the experimental approaches used to explore these aspects of lipid membranes using lipid vesicles and lipid monolayer as model membranes.

Keywords Antimicrobial peptides · Model membranes · GUVs · Lipid monolayers · Lipid-packing perturbation

This article is part of a Special Issue on 'Latin America' edited by Pietro Ciancaglini and Rosangela Itri

✉ João Ruggiero Neto
jruggiero@sjrp.unesp.br

[1] Department of Physics, UNESP - São Paulo State University, IBILCE, R. Cristóvão Colombo, 2265, São José do Rio Preto, SP CEP 15054-000, Brazil

Introduction

Antimicrobial peptides belong to the innate immune system and are part of the first line of defense of many species from bacteria to plants and humans (Nguyen et al. 2011; Wang 2014). These short sequences, with up to 40 residues, are rich in cationic and non-polar amino acids, which are distributed in the sequence in such a way that they are prone to form amphipathic structures, alpha helix or beta structures, when in adequate conditions (Zasloff 2002; Yeaman and Yount 2003). In the present review, we will focus on the helical antimicrobial peptides whose structure is formed when they are in contact with lipid membranes and/or in a specific ambient such as surfactant micelles or helix-inducing agents such as trifluoroethanol (TFE).

A wealth of information regarding the mode of action of these peptides has been gathered over recent decades (Parente et al. 1990; Matsuzaki et al. 1996a; Pokorny et al. 2002; Huang et al. 2004; Sengupta et al. 2008; Epand et al. 2009; Haney et al. 2010; Nguyen et al. 2011). Some of this information indicates that the bactericide activities of all L-residue peptides are the same as for all D-residue peptides. Neither these forms can be distinguished by bacteria (Wade et al. 1990; Chen et al. 2006). This lack of discrimination indicates that these peptides act directly on the lipid matrix of the cell membrane, with no requirement for specific membrane receptors (Hancock et al. 1995; Shai 1999; Epand and Vogel 1999;

Zasloff 2002). The outer leaflet of the plasma membrane of prokaryotic cells is rich in anionic phospholipids (Malanovic and Lohner 2015), while the surface of the eukaryotic cells is electrostatically neutral due to the dominance of zwitterionic and uncharged lipids (Rothman and Lenard 1977; Devaux 1991). Due to their cationicity, antimicrobial peptides have a preference for anionic membranes, driven mostly by electrostatic interactions between them. In addition, since they only act in the membrane lipid matrix, it is difficult for the microorganism to develop a resistance mechanism against these peptides, rendering them promising alternatives to conventional antibiotics. The search for and development of new antibiotic compounds was identified as a task of global importance in the recent O'Neil report to the United Kingdom government on the reduction of the widespread increase in microorganism resistance (O'Neill 2015). Several recently investigated cationic peptides are currently undergoing clinical trials (Marshall and Arenas 2003; Arias and Murray 2009; Yeung et al. 2011; Bahar and Ren 2013).

In the present review, we discuss the lytic activity of the antimicrobial natural peptide MP1 (IDWKKLLDAAKQIL-NH_2) and the synthetic peptide L1A (IDGLKAIWKK VADLLKNT-NH_2) and its N-acetylated analog, Ac-L1A, containing concomitantly acid and basic residues whose net charge could be modulated by changes in solution pH. The lytic activity of these peptides was explored in both large and giant unilamellar vesicles (LUVs and GUVs, respectively). The effect of these peptides on lipid packing was assessed by their impact on lipid monolayers.

The action mechanism of helical antimicrobial peptides

Several models have been proposed for the action mechanism of antimicrobial peptides, and they have been recently revised (Nguyen et al. 2011; Wimley and Hristova 2011; Bechinger 2015). Some of these models were proposed largely as a result of leakage experiments. All the models proposed to explain the action mechanism of these peptides begin with the peptide adsorption onto the lipid bilayer. In solution, the peptide is unstructured and its adsorption is followed by its folding into an amphipathic structure, mostly helix whose axis is parallel to the membrane surface. The adsorption of the peptide onto the membrane continues until a critical concentration is achieved, creating a mass imbalance and elastic stress which is relieved by forming defects or pores, leading to the lytic process. The peptide can aggregate and then form a transmembrane pore in which the hydrophobic faces of the peptides are in contact with the acyl chains, which requires that the peptide length span the bilayer thickness (Parente et al. 1990; Huang et al. 2004). Toroidal pores can be formed after the adsorbed peptide concentration achieves a critical value. In these pores the outer and the inner leaflets of the bilayer are fused and the lipids are then curved inward; these pores are toroidal holes lined by lipids and peptides (Matsuzaki et al. 1996b; Huang et al. 2004). In an alternative model, the adsorbed peptides induce curvature strain in the bilayer, which is relieved by their aggregation into the bilayer, enabling the aggregate to be translocated to the vesicle lumen by a sinking-raft process (Pokorny et al. 2002). Depending on the lipid composition of the bilayer, the peptide can induce a non-lamellar phase and be translocated across the membrane by the formation of non-bilayer intermediates in which the peptide is trapped inside inverted micelle (Haney et al. 2010). At higher peptide-to-lipid ratios, the peptides can also act as a detergent, inducing micellization of the lipid bilayer or its rupture. These mechanisms are not exclusive and a given peptide can present more than one mechanism depending on the peptide-to-lipid ratio (Bechinger and Lohner 2006). A challenging question not answered until now is how many different mechanisms exist and how many can operate at the same time (Wimley and Hristova 2011).

Irrespective of the action mechanism, the peptide is adsorbed onto the lipid bilayer, most frequently folded in an amphipathic helical structure, in which the charged and polar residues of the hydrophilic face are either in contact with the lipid head groups or solvated by the aqueous environment and the hydrophobic residues, including the backbone, seeking a water-depleted environment (Dathe and Wieprecht 1999). The amphipathic structure is relevant in peptide penetration and perturbation of the membrane leading to the lytic process. Although some peptides lack an amphipathic structure, they are still capable of disturbing the lipid packing and of inducing the lytic process by an interfacial action (Wimley 2010).

The adsorption of peptides onto anionic bilayers is mostly directed by electrostatic interactions due to their net charge being opposed to that of the target membrane. Even adsorption onto a neutral bilayer would have a small electrostatic component due to the dipolar character of the zwitterionic head-groups. When a peptide is adsorbed onto the lipid bilayer, at a low peptide-to-lipid concentration ratio, evidence has shown that its orientation is preferentially parallel to the membrane surface (Bechinger et al. 1992; Silvestro and Axelsen 2000; Marassi and Opella 2000; Klocek et al. 2009). In this orientation, the peptide inserts its non-polar face into the region between the lipid head groups and the acyl chains. The peptide is sufficiently stiff, and the highly flexible acyl chains adapt their conformation to accommodate the insertion of the peptide. This conformational adaptation of the acyl chains creates elastic distortions, resulting in a compression of the outer layer, which responds with a change in the lipid area, (ΔA). The elastic energy penalty to be paid for this change in

area is proportional to $(\Delta A/A)^2$ (Fošnarič et al. 2006). The perturbation of the acyl chains also leads to changes in their molecular packing and in the order parameter, with consequences for the thermotropic properties of the bilayer (Jing et al. 2003). In addition, if the peptide has a charge density higher than that of the bilayer, this excess of positive charges acts to recruit oppositely charged lipid head groups, inducing lipid de-mixing (May et al. 2000; Epand et al. 2010; Bagheri et al. 2015). Furthermore, overstretching the outer layer in relation to the inner layer can induce two different responses which are not exclusive: membrane thinning of the lipid bilayer, as observed by X-ray and neutron diffraction (He et al. 1995; Spaar et al. 2004), and changes in the membrane curvature (Zemel et al. 2008).

Model membranes and strategies for investigating lipid-packing perturbation

From the physical point of view, model membranes are a simple system, composed of lipids (phospholipids, sphingolipids, sterol), incorporating the most important characteristics to be investigated in the cell membrane, which is very complex (Eeman and Deleu 2010). In general, these characteristics are related to the lipid composition, lateral pressure and other features representing the targeted plasma membrane of the living system. Lipid vesicles have been shown to represent a valuable model system for the investigation of many aspects of peptide-to-lipid interactions, especially the lytic process and the thermotropic properties of lipids and phase transition in lipid bilayer (McElhaney 1982; McElhaney 1986). Lipid monolayers are another valuable model membrane which makes it possible to assess the effect of peptide on the phase transition of the lipid film, providing information on the changes of lipid packing induced by the peptide. These model membranes have been widely reviewed in the literature (Brockman 1999; Maget-Dana 1999; Birdi 2006; Dennison et al. 2010; Stefaniu et al. 2014; Wilke 2014).

Lipid vesicles for the investigation of the lytic activity of antimicrobial peptides

Large and giant unilamellar vesicles, LUVs and GUVs, respectively, have been extensively used to investigate the lytic activity of antimicrobial peptides. The preparation of large unilamellar vesicles (LUVs) is very simple and widely diffused in the literature (Hope et al. 1985; Hope et al. 1986). In brief, a lipid solution in organic solvent is deposited into a round-bottom flask, at desired composition and concentration, and is then dried by N_2 flux and subsequently under vacuum, for a few hours, to remove excess of organic solvent. The film obtained is then hydrated by gentle agitation with a solution containing a fluorescent dye, in general carboxyfluorescein or calcein, ~10 °C above the melting temperature of the lipids, forming a suspension of multilamellar vesicles (MLVs). This suspension is then submitted to several steps of extrusion through polycarbonate membranes with pores of known diameter. The non-encapsulated dye is removed by gel filtration chromatography. In leakage experiments, a fixed aliquot of the vesicle suspension is added to a solution containing a given peptide concentration. When entrapped in the vesicle, the fluorescence intensity is self-quenched. Upon the action of the lytic peptide, a fraction of the entrapped dye is released from the vesicle and the fluorescence is de-quenched, and the time course of the fluorescence intensity change is monitored. The increase in fluorescence intensity is proportional to the peptide concentration of the solution to which the vesicles are added. At each peptide concentration used, the percentage of released dye can be obtained as: % leakage = $(F - F_0)/(F_{100} - F_0)$, where F is the fluorescence intensity after a time interval of peptide action, F_0 is the fluorescence intensity in the absence of peptide, and F_{100} is the intensity obtained for entire release induced by the addition of a surfactant, in general, Triton X-100. The lytic activity is analyzed using a dose–response curve, % leakage versus peptide concentration, and by the kinetic of fluorescence intensity change due to the leakage (Jin et al. 2005; Rautenbach et al. 2006; Wang et al. 2012). Alternatively, the fluorescent dye, 8-aminonaphthalene-1,3,6-trisulfonic acid (ANTS), can be entrapped with its quencher, *p*-xylenebis-pyridinum bromide (DPX), and, upon release, it can be re-quenched by further addition of the quencher (Yandek et al. 2009). This method allows the amount of dye released and the amount that remained entrapped after the peptide action to be monitored. With this alternative experiment, it is possible to estimate whether the leakage process is graded or all-or-none (Parente et al. 1990; Pokorny et al. 2002). In addition, Heerklotz and coauthors (Patel et al. 2009) developed a method using time-resolved fluorescence approach to monitor dye release (calcein) from LUVs. This method provided evidence about the heterogeneity of graded leakage and also allowed distinguishing from all-or-none leakage process.

Giant unilamellar vesicles (GUVs) can be formed either by spontaneous formation (Akashi et al. 1996) or by electroformation (Angelova and Dimitrov 1986), and have been extensively reviewed in the literature (Yamazaki and Tamba 2005; Dimova et al. 2006; Riske 2015). Briefly, in spontaneous formation, after the solvent has been completely removed by vacuum, the lipid film, whether or not it contains fluorescently labeled lipid, is pre-hydrated with a very small volume of water (~10 μl) at 45 °C for a short time, ~10 min. This pre-hydrated film is incubated with a sucrose solution, with or without a fluorescent dye, at 37 °C overnight, and a visible cloud, containing the GUVs, is formed. In the electroformation method, the lipid solution

is deposited on the conductive sides of two glass plates covered with indium tin-oxide or alternatively over two parallel platinum electrodes (wires) (Puff and Angelova 2006). The surfaces of the conducive plates containing the lipid film will be the inside walls of a chamber formed by the plates and a rectangular Teflon separator. In both approaches, the lipid film is hydrated with the sucrose solution and the electrodes are connected to a pulse generator, and a low AC voltage (1–3 V) at frequency of up to 10–20 hertz is applied for 2–3 h. The electric field induces the lipid layer to peel off, followed by self-assembly leading to vesicle formation. Where the GUVs are grown with a fluorescent dye and sucrose solution, the excess of dye outside the GUVs must be removed by gel filtration (Tamba et al. 2011; Islam et al. 2014). Aliquots of the harvested GUVs are diluted in an equal osmolarity glucose or buffer solution. The difference between the refractive indices of the outside and the inside solutions of the GUVs enables the vesicles to be visualized by phase contrast microscopy. For dye-encapsulated GUVs, the leakage process can be monitored by fluorescence microscopy (FM). The spontaneous formation and electroformation are the most common approaches to growing GUVs. These methods present the same limitations when large amount of negatively charged lipids and high ionic strength are used. Recently, Weinberger and collaborators (Weinberger et al. 2013) developed a new methods in which GUVs grown on a polyvinyl alcohol film, allowing the formations of GUVs in different aqueous solution and large range of lipid composition.

The peptide is then injected into the GUV suspension in the observation chamber (which contains an optical window) using a glass micropipette connected to a micromanipulator. The experiment is then monitored by phase contrast or fluorescence microscope connected to a CCD camera. Alternatively, this experiment can be performed by adding GUVs to a solution of one or more fluorescent dyes, and the influx into the vesicle lumen can be monitored by FM (Leite et al. 2015; Alvares et al. 2017), enabling the lytic activity for single vesicles to be obtained.

GUV observations provide specific information about the lytic activity of peptide for a single vesicle, such as shape deformation and vesicle rupture, that cannot be obtained by experiments in LUVs. However, in GUV experiments, it is not possible to control the lipid concentration, and the lipid-to-peptide ratios cannot be exactly determined. In addition, LUV experiments provide information about leakage from a collection of vesicles while, in experiments with GUVs, the information obtained is for a single vesicle. The two techniques thus complement each other describing the lytic activity of peptide. Here, we demonstrate that it is possible to distinguish between graded and all-or none leakage mechanisms in GUVs and LUVs and that they coincide in both methods.

The effect of lipid composition on affinity and lytic activities in vesicles

The adsorption of lytic peptide to the membrane creates an elastic stress, as described above. It may therefore be expected that the composition of the lipid bilayer will play an important role in peptide action. In addition to potent and broad-spectrum bactericide activity, the peptide Polybia-MP-1 (MP1) also inhibited the proliferation of prostate and bladder cancer cells (Wang et al. 2008) and, in lymphocytes, proved to be multidrug resistant (Wang et al. 2009). It was observed that this peptide selectively recognized leukemic T-lymphocytes and not healthy ones, being harmful only to leukemic ones (Dos Santos Cabrera et al. 2012). Cancer cells lose the asymmetric lipid distribution of healthy cells with the aminophospholipids phosphatidylserine (PS) and phosphatidylethanolamine (PE) in the inner layer, and phosphatidylcholine (PC) and sphingomyelin (SM) in the outer layer of the membrane. The asymmetrical phospholipid distribution observed in healthy human cells is maintained by the family of enzymes aminophospholipid translocases (Devaux 1992). In cancer cells, the aminophospholipids are exposed in the outer leaflet (Utsugi et al. 1991; Fadok et al. 1992, 1998; Stafford and Thorpe 2011), rendering their surface negatively charged, which can be discriminated by cationic peptides. The effect of PS and PE on the lytic activity of MP1 was explored in GUVs and LUVs composed of pure DOPC, DOPC/DOPE (9:1), DOPC/POPS (8:2) and DOPC/DOPE/POPS (7:1:2). In GUV experiments, a GUV suspension was added to a solution containing three different dyes: carboxyfluorescein (CF), cascade-blue-labeled dextran (3 k–CB) and Alexafluor dextran (10 k–AF647), with molecular weights of 0.36, 3.0 and 10.0 kD, respectively; the influx to the vesicle lumen was monitored by FCM. In addition, a small fraction (~0.5 mol%) of DOPE-rhodamine was used to check the bilayer integrity during the peptide action. The dye concentration inside the GUV, at a given time t, was calculated by: $c(t) = (p_{in,\,t} - p_{in,\,control})/(p_{ex,\,t} - p_{ex,\,control})$, where $p_{in,t}$, $p_{in,control}$, $p_{ex,t}$ and $p_{ex,\,control}$ are the pixel intensity inside the GUV at time t, inside at time zero, outside the GUV at time t and outside at time zero, respectively. The kinetics of dye influx (dye concentration inside the vesicle, c(t), as a function of time) of the three permeating molecules, induced by 4 μM of MP1 in PC/PE and PC/PE/PS GUV showed the existence of a time-lag in initiating the entrance of dye into the vesicle lumen that was dependent on vesicle lipid composition (see fig. S2 in Leite et al. 2015). The average time-lag calculated for 50 vesicles was smaller for the GUVs containing PS and PE, ~760 ± 120 for PC/PE/PS, compared to PC/PE, ~1600 ± 60 s, and the two other compositions (Leite et al. 2015). The increase in dye concentration in the vesicle lumen, after the time-lag, was dependent on the dye size; for PC and PC/PS vesicles, only the smallest dye achieved the complete filling. In contrast, in GUVs containing PE, the entrance of the three dyes reached complete filling even for 10 k–AF647. The dose

response curves (% of filled vesicles by dyes as a function of peptide concentration) showed that the influx of the dyes induced by MP1 was also dependent on the peptide concentration These plots show that complete filling with the smaller and even with the 10-kD dyes was only achieved in the GUVs of PC/PE/PS (see fig. S1 in Leite et al. 2015). Lytic activity decreased in the following order of lipid composition for both dyes: PC/PE/PS > PC/PE > PC/PS > PC. The histograms for CF and 10 k–AF647 influxes in 50 GUVs of pure PC, PC/PS, PC/PE and PC/PE/PS upon addition of 4.0 μM of MP1 are shown in Fig. 1a. The dye entrance or the percentage of vesicle filling was enhanced by the presence of anionic lipid. Interestingly, in the presence of PE in the binary mixture, PC/PE, almost 100% of the analyzed GUVs were totally filled. Another important observation is that the dye entrance was observed mostly in two ranges, smaller than 20% and larger than 80%, suggesting an all-or-none process of dye influx. The experiments in LUVs using the re-quenching of ANTS and its quencher DPX entrapped in the vesicles with the same lipid composition made it possible to determine the amount of ANTS remaining inside the LUVs (Q_{in}) after the peptide action and the fraction of dye released (f_{out}). These two factors, displayed in Fig. 1b, show that the amount of ANTS remaining inside LUVs is constant as the fraction of dye released increases, supporting an all-or-none process. These results provided strong evidence that the aminophospholipids PS and PE act synergistically, enhancing the permeability induced by MP1 in lipid vesicles.

In addition to the asymmetry of phospholipid distribution in their membranes, human cells also present planar ordered domains composed of sphingomyelin and cholesterol (lipid rafts) that are important for the membrane proteins and for elastic control of the membrane (Quinn 2010; Rosetti et al. 2017; Sezgin et al. 2017). Evidence has been gathered indicating that the presence and integrity of lipid rafts is necessary to maintain PS exposure (Ishii et al. 2005). The lytic activity of MP1 was investigated in GUVs containing PS and brain sphingomyelin (bSM) and cholesterol (Chol) not necessarily organized in liquid ordered domains (L_o). The experiments with GUVs examined the influx of carboxyfluorescein induced by 2 μM of peptide to the lumen of GUVs composed of pure DOPC, DOPC:POPS (4.9:2.1), DOPC:bSM:Chol (3:3:1), DOPC:POPS:bSM:Chol (2.1:0.9:3:1, L_o domains are observed) and POPC:POPS:bSM:Chol (2.1:0.9:3:1,L_o

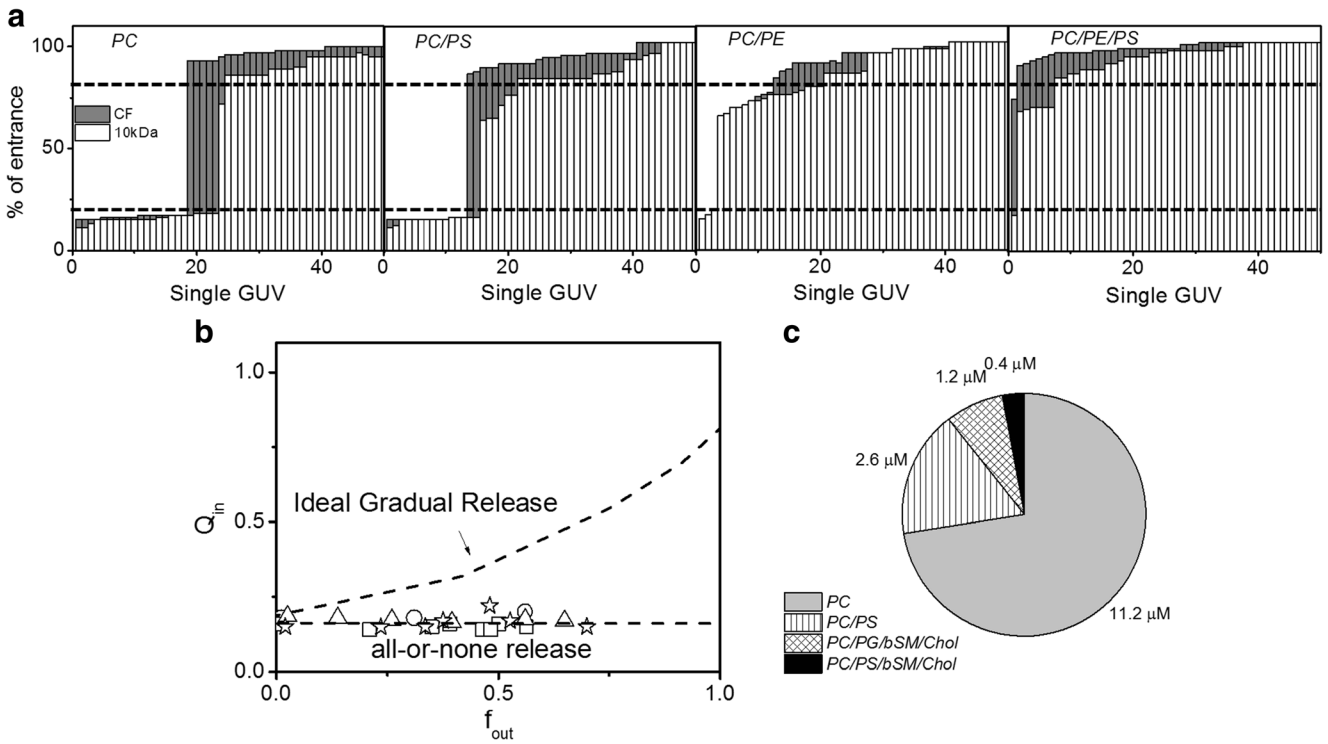

Fig. 1 Lytic activity in LUVs and GUVs modulated by the vesicle lipid composition. **a** Percentages of carboxyfluorescein (*CF*) and Alexa 647-10 k (*10 kDa*) entrance induced by MP1 in 50 individual GUVs after 30 min of addition of 4 μM of the peptide. *Horizontal dashed lines* show two ranges, 80 and 20%, defining all-or-none dye entrance. **b** ANTS/DPX re-quenching experiments monitoring leakage induce by MP1 from LUVs of pure DOPC (*circles*), DOPC/POPS (8:2) (*squares*), DOPC:DOPE (9:1) (*triangles*) and DOPC:DOPE:POPS (7:1:2) (*stars*) induced by MP1: the amount of ANTS remained in the LUVs (Q_{in}) as a function of the released ANTS fraction (f_{out}). *Dashed lines* represent the theoretical curves for ideal graded and all-or-none dye release calculated as shown in (Ladokhin et al. 1995). **c** The amount of MP1 necessary to induced 50% of carboxyfluorescein from a suspension of LUVs after 1 min of peptide/vesicles incubation. Each slice represents the composition of the LUVs: DOPC, DOPC:POPS (4.9:2.1), DOPC:POPS:bSM:Chol (2.1:0.9:3:1) and DOPC:POPG:bSM:Chol (2.1:0.9:3:1). (**a**) and (**b**) were adapted, with permission, from Leite et al. (2015)

domains are not observed) containing a small fraction (0.2 mol%) of the fluorescent lipid BodipyTR-Ceramide for the control of bilayer integrity. MP1 either failed to induce or induced only a marginal CF influx in DOPC and DOPC/bSM/Chol. The dye influx kinetic in PS-containing GUVs induced by 2 μM of MP1 showed that in DOPC/POPS GUVs, CF influx achieved 40% in ~1300s, while, in vesicles containing PS and L_o domains, only 160 s was necessary for the peptide to induce 100% of filling. Interestingly, in POPC/POPS/bSM/Chol in which liquid-ordered/liquid-disordered phase coexistence was not observed, the CF influx achieved 40% in ~1600 s (Alvares et al. 2017). The leakage experiments performed with LUVs point to results similar to those observed in the experiments with GUVs. The pie chart in Fig. 1c shows that the peptide concentration required to achieve 50% of leakage (EC_{50}) in DOPC:POPS:bSM:Chol was 6.5 and 28-times smaller compared to DOPC:POPS and DOPC LUVs, respectively, indicating that, when PS and L_o domains are present in the lipid composition, the permeability efficiency of MP1 enhanced significantly. On the other hand, when POPS was replaced by the same amount of phosphatidylglycerol (POPG), the EC_{50} was 3-times higher than the concentration observed in the presence of POPS, suggesting that, in addition to the polar head net charge, its structure seems to play an important role in peptide/lipid interaction. These results suggest a synergy between PS and liquid ordered domains in significantly influencing the lytic activity of MP1.

Charge effect on the affinity and lytic activity of peptides in lipid vesicles

Lysines (Lys) and arginines (Arg), with a positive electrical charge in physiological pH, are the aminoacid residues in antimicrobial peptides which, together with hydrophobic and non-polar residues (Fjell et al. 2012), occur to the greatest extent. Besides these positively charged residues, some natural peptides present a post-translational modification in the C-terminus that removes its negative charge, the most frequent modification being amidation (Andreu and Rivas 1998; Yeaman and Yount 2003). This C-terminal protection prevents proteolytic digestion of the peptide and has been shown to play an important role in the peptide structure. From the structural point of view, the C-terminus amidation was shown by NMR to provide an extra hydrogen bonding in Eumenine mastoparan-AF (EMP-AF-NH_2) compared with the non-amidated analog (Sforça et al. 2004). Similar observations were carried out for Protonectarina-MP using hydrogen deuterium exchange and mass spectrometry (da Silva et al. 2014). This helical stabilizing effect was also observed in the less frequent post-translational modification in the N-terminus, for instance its acetylation. Conformational analysis of the synthetic peptide L1A and its acetylated analog by molecular dynamics simulations associated with CD spectroscopy have shown that N-terminus acetylation provides four extra backbone hydrogen bonds, enhancing helical stability (Zanin et al. 2016). In addition to structural effects, these post-translational modifications of C- and N-termini result in changes in the peptide net charge. In this sense, amidation changes the C-terminus from negative to neutral under physiological conditions providing the peptide with an extra positive charge. Acetylation, on the other hand, renders the charged amino-group neutral, reducing the cationicity of the peptide. These modifications have been shown to play an important role in lytic activity in model membranes and in their biological activities. For instance, the amidation of the C-terminus of Eumenine mastoparan-AF (EMP-AF-NH_2), enhances several times the leakage efficiency induced in 7POPC:3POPG LUVs compared with EMP-AF-OH (Dos Santos Cabrera et al. 2004). Notwithstanding the net charge reduction in the acetylation of the synthetic peptide, L1A, the modified peptide showed higher efficiency in lytic activity in the mixed anionic lipid vesicle (8POPC:2POPG); EC_{50} decreased by 30% compared to non-acetylated L1A (Zanin et al. 2016). The peptide net charge can also be changed by residue substitution. MP1 is a potent antimicrobial peptide with 2 aspartic acids and 3 lysines which, with the amidated C-terminus, results in a net charge of +2. The substitution of aspartic acid (Asp) by an asparagine residue increases its net charge to +3. The increase in the net charge improved the leakage efficiency in anionic mixed LUVs and GUVs (Dos Santos Cabrera et al. 2011; Leite et al. 2011). The net charge of peptides concomitantly containing acidic and basic residues, Asp and Lys like MP1 and L1A, can be modulated by changes in the pH of the solution. The pKa of the aspartic acid, lysine and N-terminus are 4.0, 10.4 and 8.0, respectively (Grimsley et al. 2009). At a given pH, the protonation of these groups may or may not be favored by the surface electrostatic potential (ψ_0) of the vesicle. In general, the fraction of the protonated group is given by:

$$f_{AH} = \left[1 + 10^{\left(pH + 0.434\frac{F\psi_0}{RT} - pK_a\right)}\right]^{-1}$$

where F is the Faraday constant and RT is the thermal energy.

In the presence of POPC:POPG (8:2) vesicles, in which surface potential was $\psi_0 = -27.0$ mV determined from the zeta potential measurements, the calculated net charges for L1A are 3.7, 3.0 and 1.9 at pH 4.0, 7.0 and 10.0, respectively. These changes in peptide net charge had a strong effect on peptide lytic activity in anionic mixed LUVs, as shown in the dose–response curves for POPC:POPG (8:2) vesicles after 5 min of peptide action in Fig. 2a. Complete leakage was only achieved at pH 10.0, when the N-terminus and some lysines

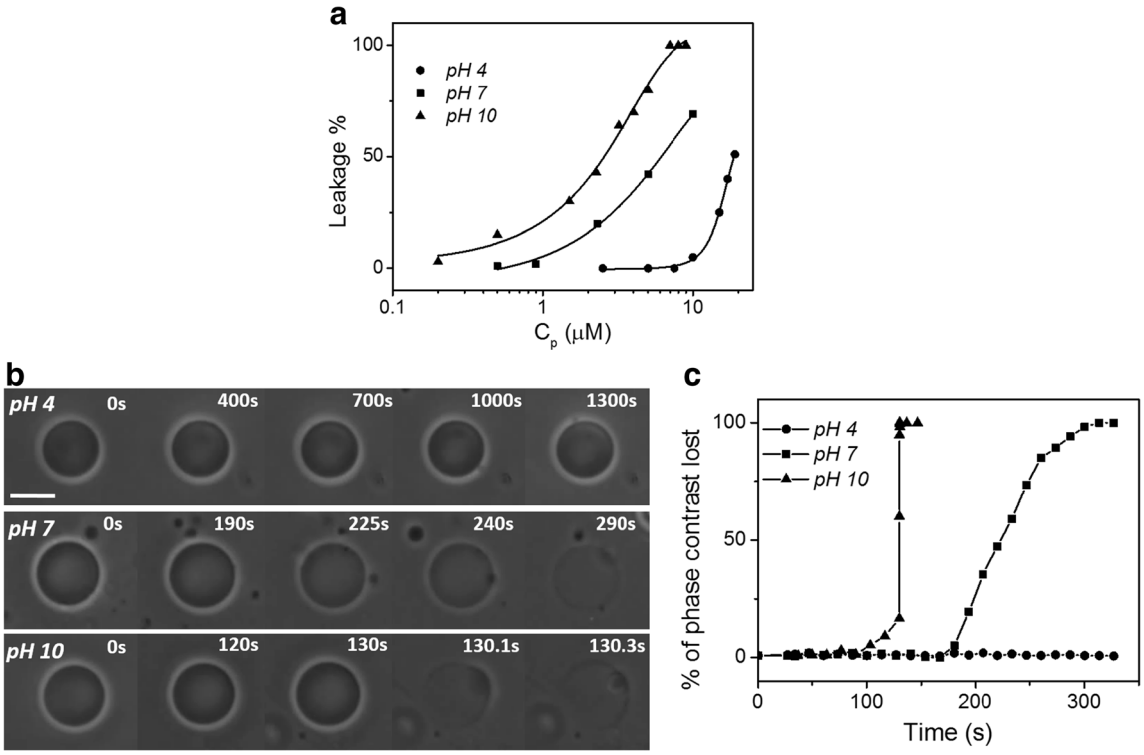

Fig. 2 The effects of pH on lytic activity induced by a pH-responsive peptide in LUVs and GUVs: **a** Dose–response curves of L1A-induced leakage of calcein from LUVs of POPC:POPG (8:2) at pH 4 (*circles*), 7 (*squares*) and 10 (*triangle*). The percentage of dye leakage after 5 min of peptide addition was plotted as a function of peptide concentration. The data were fitted with Boltzmann sigmoidal equation in order to calculate the EC_{50}. **b** Phase contrast images of POPC:POPG (8:2) vesicles after addition of 7 μM of L1A showing the effect of solution pH on lytic activity of the peptide. The peptide was continuously injected near a single GUV using a glass micropipet controlled by a micromanipulator (Narishige, Tokyo, Japan). The time indicated on the first image represents the start of peptide injection. *Scale bar* 20 μm. **c** pH effect on the kinetics of sucrose/glucose permeability from a single GUV induced by L1A shown in (**b**) as a function of time

were deprotonated. The values of EC_{50} in the anionic mixture were 17, 6 and 2 μM at pH 4.0, 7.0 and 10.0, respectively. Similar observations were also made in experiments with GUVs. The effect of peptide was investigated by monitoring changes in phase contrast. Figure 2b shows phase contrast snapshots of 8POPC:2POPG GUVs before and after the injection of 7 μM of L1A near the GUVs in different pH solutions. In both neutral and basic pH, the peptide induced a complete loss of phase contrast; however, the kinetic was dependent on the pH of the solution (see Fig. 2c). At pH 7, the loss of contrast was gradual and the time to complete contrast loss was 1.8-times higher than at pH 10.0. At pH 10.0, a quick lytic process took place, only 130 s after peptide injection, and vesicle burst was observed after complete loss of contrast for all the analyzed GUVs. On the other hand, L1A did not induce permeability after a long time of peptide injection (1800 s) when the experiments were performed at pH 4.0. These results indicate that the neutralization of the N-terminus charge favors lytic activity probably by inducing higher perturbation in lipid packing. In fact, this result is in good agreement with the results obtained for the acetylated analog of L1A (Zanin et al. 2013, 2016).

Charge effect on lipid packing perturbation induced by peptides in lipid monolayer

The Langmuir monolayer, a model system that mimics a single leaflet of the bilayer, has been extensively used to investigate lateral lipid–lipid interactions, as well as the impact of antimicrobial peptide on lipid packing (Fischer et al. 1984; Worthman et al. 1997; Eeman et al. 2006; Neville et al. 2006; Bouffioux et al. 2007; Dennison et al. 2008; Wilke 2014). The main advantage of this system is that the molecular density and lipid composition can be varied without limitation, while the pressure–area isotherms are monitored by simultaneous visualization of the monolayer with microscopy techniques (Lösche et al. 1983; Henon and Meunier 1991; Möhwald 1995; Kaganer et al. 1999; Lheveder et al. 2000).

A lipid film can be formed by spreading a lipid solution, in organic solvent, on an air–aqueous interface (Kaganer et al. 1999). Due to its amphiphilic characteristic, a monomolecular film, in which the polar head-groups are in contact with water and the acyl chains are in the air (low dielectric constant phase), can be formed in a Langmuir trough containing two movable barriers whose position is controlled by a servomechanism

(Maget-Dana 1999). The movement of these barriers applies a lateral surface pressure on the lipid film while the surface tension is monitored by a Wilhelmy plate connected to a microbalance. As the surface pressure increases, the area available to the lipid molecules decreases, resulting in a pressure–area (π vs. A) isotherm. The packing and orientation of the hydrophobic tails of the lipid molecules change during the compression, giving rise to phase transitions from a loosely unordered gas-like phase to a liquid phase or to a highly ordered condensed phase, similar to a 2-D vant'Hoff isotherm. Some lipids present both the liquid-expanded (LE) and the liquid-condensed (LC) phases and a plateau of coexistence of these phases (Fischer et al. 1984). In the phase coexistence region, solid domains are formed and grow during the compression of the lipid film (Heckl et al. 1986; Miller and Mohwald 1987; Vanderlick and Möhwald 1990). The separate phases and the morphology of these solid domains can be visualized by FM (Lösche et al. 1983; Weis and McConnell 1984; Mohwald 1990) or Brewster angle microscopy (BAM) (Hoenig and Moebius 1991; McConlogue and Vanderlick 1997; Mottola et al. 2013) during film compression or by atomic force microcopy (Clausell et al. 2004; Mularski et al. 2015) in films transferred to a solid substrate at a given surface pressure (Mangiarotti and Wilke 2015). The pressure at which the phase coexistence takes place and the extension of the plateau are very sensitive to the pH, ionic conditions and temperature of the subphase (Mohwald 1990; Maltseva et al. 2006; Vega Mercado et al. 2011). This plateau of coexistence is an important signature to be used in the investigation of the impact of a peptide on lipid packing (Dennison et al. 2014). The interfacial properties of antimicrobial peptides also influence peptide/lipid interaction. Surface pressure–area isotherms of pure peptide provide useful information about its capability to form monolayers, and the possible orientation of the peptide in the monolayer. Through the compression curves, two important values can be obtained: the collapse surface pressure, π_{col}, and the limiting molecular area, A_{Lim}. π_{col} is the surface pressure at which the film collapses and, A_{Lim} is the minimal area before the collapse. In this context, compression isotherms of pure L1A were carried out in saline solution at pH 2, 4, 7 and 10. The values of π_{col} and A_{Lim} indicated that L1A, as well as MP1, was able to form a stable monolayer at the air–aqueous interface, adopting a mostly α-helical conformation oriented almost perpendicularly to the interface (for details of calculation, see (Alvares et al. 2016)). This orientation was also reported for other surface active peptides (Ambroggio et al. 2004; Mura et al. 2013). Figure 3a, b shows how the π_{col} and A_{Lim}, respectively, are affected by the subphase pH. At pH 2, the peptide was totally protonated and the repulsion between the high net charge peptides led to an unstable peptide film characterized by the lower collapse surface pressure. At pH 4, the aspartic acids were partially protonated, and, despite the reduction of the peptide net charge, a repulsive peptide-peptide interaction prevailed. At neutral pH, both kinds of charged amino acids were charged and, despite the ionic strength, salt bridges were able to form, resulting in a more stable film compared to acidic pH. At basic pH, where the N-terminus and the lysines were totally and partially deprotonated, respectively, the repulsion between peptide molecules was reduced, leading to the formation of a stable peptide film of the highest lateral pressure (see Fig. 3a). The collapse pressure was a function of the pH of the solution and, consequently, of the peptide net charge. The dependence of collapse pressure and limiting molecular area on the subphase pH was also observed in other peptides, such as MP1 (Alvares et al. 2016), melittin (Fidelio et al. 1986) and maculatin (Ambroggio et al. 2004).

In the investigation of the impact of the peptide on lipid packing, it was important to use a lipid monolayer with a lipid that displays the LE–LC coexistence plateau, like, for instance, DPPC, co-spread with the peptide. The impact of MP1 on the phase behavior of the DPPC monolayer at acidic and basic pH was analyzed using BAM (Alvares et al. 2016). At acidic pH, MP1 induced the formation of smaller and more rounded LC domains compared to all other conditions. In the classical nucleation process of a system, the number of nuclei increases when the compression rate increases or when the lipid diffusion decreases (Bernchou et al. 2009; Vega Mercado et al. 2012). The change in domain size/shape may be attributed to a more viscous monolayer at acidic pH than at basic and neutral pHs. In the case of neutral and basic pHs, the domains presented triskelion-like shapes similar to those formed by pure DPPC films at the same subphase condition. In acidic, neutral and basic solutions, the peptide remained in the liquid-expanded phase and the liquid-condensed domains were composed of nearly pure lipid. Similar effects were also observed for DPPC/L1A monolayers. Figure 3c shows the FM images obtained for DPPC/L1A monolayers at pH 4 and 10. Due to the similitude of L1A and MP1, a similar explanation can be given for the changes in the shape/size of domains induced by L1A. These results show that the pH of the subphase is an important parameter that modulates the surface activity of the peptide, emphasizing the importance of lateral interaction between peptide molecules to stabilize the peptides in the hydrophobic region in the membrane.

pH effect on the surface activity of peptide and its insertion into lipid monolayers

The surface activity of peptide can also be investigated by experiments on a constant area monitoring the adsorption kinetics of peptide at a clean interface (without lipid) (Maget-Dana et al. 1999; Ambroggio et al. 2006; Eeman et al. 2006; Dennison et al. 2009). The progress of the adsorption depends on ionic strength, pH, temperature and peptide concentration (Seelig 1990; Maget-Dana 1999; Dennison et al. 2010). The influence of both the peptide concentration and pH are shown in Fig. 3d for the peptide L1A. As can be clearly seen,

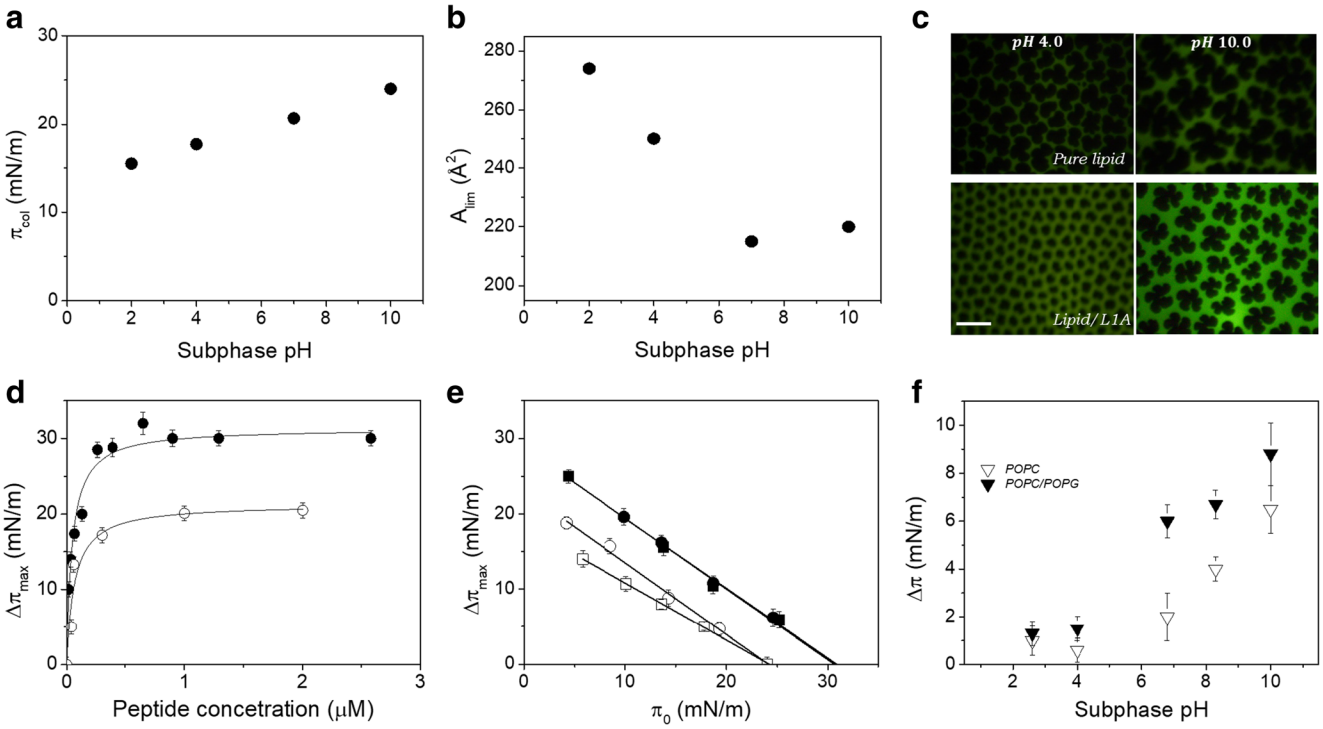

Fig. 3 pH effect on the perturbation of lipid packing induced by L1A in lipid monolayer. **a**–**c** Pressure-area isotherm experiments: **a** collapse pressure (π_{col}) and **b** limiting molecular area (A_{Lim}) of pure L1A in saline solution as a function of the subphase pH. **c** Representative FM images of pure DPPC and DPPC/L1A for X_{L1A} = 0.048 monolayers, spread onto a saline solution at pH 4 and 10, obtained at a surface pressure of 7 mN/m. The monolayer contained 0.5 mol% of fluorescent lipid NBD-PC. *Scale bar* 50 μm. **d**–**f** Constant area assay: **d** the maximum change of surface pressure ($\Delta\pi_{max}$) as a function of peptide concentration injected on a saline solution at pH 4 (*open circles*) and pH 10 (*closed circles*). The *continuous lines* represent the non-linear least-squares regression analysis: $\Delta\pi = \frac{c\Delta\pi_{max}}{c+K}$, where c is the peptide concentration, π_{max} is the maximum surface pressure achieved and K is a peptide concentration that reaches half $\pi_{max.}$ **e**, **f** Peptide insertion into lipid monolayers with depth-dependence polar head group, lipid packing and pH: $\Delta\pi_{max}$ after injection in the subphase of 1.25 μM L1A measured (**e**) as a function of initial pressure (π_i) of DPPC (*circles*) and DPPG (*squares*) monolayers at pH 4 (*open symbols*) and pH 10 (*closed symbols*) and (**f**) as a function of subphase pH of POPC (*open triangles*) and 8POPC:2POPG (*closed triangles*) at π_i of 30 mN/m. *Continuous lines* in (**e**) represent the linear regressions. All experiments were performed in 150 mM NaCl solution at a constant temperature, 20 °C

0.25 μM of peptide is necessary to achieve the highest surface pressure change at basic pH while, at pH 4.0, the concentration was higher, ~1.0 μM. The peptide displayed higher surface activity at pH 10 than pH 4 (30 and 20 mN/m, respectively). In the latter condition, the aspartic acids are partially neutralized and, when peptide molecules adsorb, a more repulsive peptide–peptide interaction profile prevails, destabilizing the film and impairing the integration of new molecules. At pH 10, near the isoelectric point, the integration of new molecules into the film was not hindered (Maget-Dana 1999). Interestingly, the surface pressure achieved from peptide adsorption was higher than the collapse pressure of pure peptide Langmuir films (see Fig. 3a, d). Regarding the differences between these films, the maximal surface pressure reached in adsorption experiments might not be similar to the collapse pressure obtained from compression isotherms, but the behavior of the peptide can be compared. The peptide monolayer that is formed from adsorption is in equilibrium with molecules present in the subphase, in opposition, when the film is formed spreading the molecules directly at the air–aqueous interface corresponds to an out-of-equilibrium process (Maget-Dana 1999).

The surface pressure is sensitive to the perturbation induced by peptide in the lipid packing and can be carried out by monitoring the peptide insertion into lipid monolayer. An experiment can be performed by keeping the film pressure constant and monitoring the increase in area of the lipid film (1) or by keeping the area constant and measuring the change in the surface pressure (2).

These experiments make it possible to compare the ability of peptide to interact with lipid monolayer with different charges and packing (Hädicke and Blume 2016). In brief, the lipid monolayer is formed at a desired surface pressure, by spreading a small drop of lipid solution in chloroform (or chloroform/methanol mixture) at the air–aqueous interface, and the peptide solution is then injected into the subphase under constant stirring. The insertion of the peptide into the monolayer is accompanied by an increase in the area of lipid molecule (ΔA) or by an increase in the surface pressure ($\Delta\pi$)

as a function of time. For both experiments, the surface pressure chosen is, normally, 30 mN/m, which is the value of lateral pressure at which bilayers and monolayers can be compared (Marsh 1996).

Arouri et al. (2011) performed experiments at a constant pressure in order to study the insertion of the antimicrobial synthetic peptide KLA1 into lipid monolayers, investigating the effect of the surface charge density and the phase state. These results showed that the peptide induced change in ΔA only in anionic lipid monolayer (POPG and DPPG). With regard to the lipid phase state, KLA1 penetrated faster into the liquid-expanded POPG monolayer compared to the more compact DPPG monolayer, inducing greater change in the ΔA.

In constant area experiments, the pressure at which equilibrium is reached was observed to be linearly dependent on the initial pressure (π_0). Extrapolating the plot $\Delta\pi$ versus π_0 to $\Delta\pi = 0$ mN/m, the saturation pressure, π_s, is determined (Maget-Dana 1999; Boisselier et al. 2017). This pressure is the maximal pressure at which the peptide is able to penetrate into the monolayer and can be used to estimate the capacity of peptides to penetrate target cell membranes (Brockman 1999). Travkova and Brezesinski (2013) have studied the penetration of C/S-Ar-1, a cationic antimicrobial peptide, into zwitterionic (POPC, DPPC) and anionic (POPG, DPPG) lipid monolayers with different lipid packing. The values of π_s indicated that the extent of the insertion of the peptide varies in the order: POPG > DPPG ≅ DPPC > POPC. As expected, the cationic C/S-Ar-1 interacted preferentially with anionic lipid compared to zwitterionic lipids. The packing of the lipid is thus also reflected in the perturbation induced by peptide. In the subphase containing high ionic strength (150 mN NaCl) and neutral pH, POPG displays a liquid expanded phase in the range of initial pressure, while DPPG presents a LC phase at a pressure higher than 10 mN/m. In the LC phase, the acyl chain can be more closely packed, impairing the peptide insertion. Dennison et al. ((2007) investigated the impact of anionic lipid on the ability of Aurein 1.2 peptide to insert itself into the lipid monolayer formed by DMPC/DMPS and DMPC/DMPG with a different molar ratio. The results showed that the presence of anionic lipid was necessary for peptide to induce larger change in the surface pressure, and that the structure of the head group of anionic lipids did not affect this effect. At constant pressure, using the same lipid monolayer compositions, aurein 1.2 induced an increase in the area per lipid molecule only in the presence of negatively charged lipid. The results indicated that aurein 1.2/membrane interaction is promoted by the presence of anionic lipid.

In addition to the effects of surface charge and lipid packing, the perturbation induced by the peptide on the lipid monolayer is also dependent on the subphase pH. The insertion of L1A into DPPC and DPPG monolayers were investigated at pH 4 and 10. As seen in Fig. 3e, the values of π_s induced by L1A were similar to the maximal surface pressure achieved when the peptide was adsorbed into a clean surface at both pHs, indicating that the peptide might accumulate close to the head groups without being incorporated into the monolayers. At an initial surface pressure of 30 mN/m, L1A induced higher change in the surface pressure at pH 10 compared to pH 4 in both the POPC and 8POPC:2POPG monolayers, indicating the greater ability of peptide to penetrate into liquid-expanded phase and to induce perturbation in the lipid packing at basic pH.

Concluding remarks

Lytic peptides with bactericidal activity are highly active in the lipid matrix of the cell membrane being selective to the anionic membrane. In addition to the electrostatic interaction driving the association of these peptides to the surface of the anionic lipid bilayers, their efficiency in disturbing the lipid packing is directly related to their ability to promote the lytic process and cell lysis. Evidence gathered in the present review shows that the perturbations induced by the peptides in lipid vesicles are modulated by the lipid composition and peptide sequence. Electrostatic and hydrophobic interactions were shown to play an important role in the adsorption of pH-responsive peptides whose net charge can be modulated by the pH of the solution. The concomitant presence of acidic and basic residues in these peptides and their ionization states are strongly related to their capability to disturb the lipid packing of bilayers and monolayers. The association of the experimental techniques focused in the present work led to an understanding of some aspects of the initial steps related to the lytic process of these peptides.

Acknowledgments The authors acknowledge financial support from São Paulo Research Foundation - FAPESP (J.R.N. Grants #2015/25619-9 and D.S.A has a post-doctorate fellowship, grants #2015/25620-7). J.R.N. is a researcher for Brazil's National Council for Scientific and Technological Development (CNPq). T.G.V. has a PhD fellowship from CNPq. DSA thanks UNESP and CAPES for former scholarships. The authors thank Dr. Paul Andrew Beales from the University of Leeds (UK) and Dr. Ernesto E. Ambroggio from the University of Cordoba (Argentina) with whom the FCM experiments were performed in collaborative projects.

Compliance with ethical standards

Conflicts of interest Dayane S. Alvares declares that she has no conflicts of interest. Taisa Giordano Viegas declares that she has no conflicts of interest. João Ruggiero Neto declares that he has no conflicts of interest.

Ethical approval This article does not contain any studies with human participants or animals performed by any of the authors.

References

Akashi K, Miyata H, Itoh H, Kinosita K (1996) Preparation of giant liposomes in physiological conditions and their characterization under an optical microscope. Biophys J 71:3242–3250

Alvares DS, Fanani ML, Ruggiero Neto J, Wilke N (2016) The interfacial properties of the peptide Polybia-MP1 and its interaction with DPPC are modulated by lateral electrostatic attractions. Biochim Biophys Acta Biomembr 1858:393–402

Alvares DS, Ruggiero Neto J, Ambroggio EE (2017) Phosphatidylserine lipids and membrane order precisely regulate the activity of Polybia-MP1 peptide. Biochim Biophys Acta Biomembr 1859:1067–1074

Ambroggio EE, Separovic F, Bowie J, Fidelio GD (2004) Surface behaviour and peptide-lipid interactions of the antibiotic peptides, Maculatin and Citropin. Biochim Biophys Acta Biomembr 1664: 31–37

Ambroggio EE, Villarreal MA, Montich GG et al (2006) Interfacial properties of the M1 segment of the nicotinic acetylcholine receptor. Biophys Chem 121:171–176

Andreu D, Rivas L (1998) Animal antimicrobial peptides: an overview. Biopolymers 47:415–433

Angelova MI, Dimitrov DS (1986) Liposome electroformation. Faraday Discuss Chem Soc 81:303–311

Arias CA, Murray BE (2009) Antibiotic-resistant bugs in the 21st century — a clinical super-challenge. N Engl J Med 360:439–443

Arouri A, Kerth A, Dathe M, Blume A (2011) The binding of an amphipathic peptide to lipid monolayers at the air/water interface is modulated by the lipid headgroup structure. Langmuir 27:2811–2818

Bagheri A, Taheri-Araghi S, Ha BY (2015) How cell concentrations are implicated in cell selectivity of antimicrobial peptides. Langmuir 31: 8052–8062

Bahar A, Ren D (2013) Antimicrobial peptides. Pharmaceuticals 6:1543–1575

Bechinger B (2015) The SMART model: soft membranes adapt and respond, also transiently, in the presence of antimicrobial peptides. J Pept Sci 21:346–355

Bechinger B, Lohner K (2006) Detergent-like actions of linear amphipathic cationic antimicrobial peptides. Biochim Biophys Acta Biomembr 1758:1529–1539

Bechinger B, Zasloff M, Opella SJ (1992) Structure and interactions of magainin antibiotic peptides in lipid bilayers: a solid-state nuclear magnetic resonance investigation. Biophys J 62:12–14

Bernchou U, Ipsen JH, Simonsen AC (2009) Growth of solid domains in model membranes: quantitative image analysis reveals a strong correlation between domain shape and spatial position. J Phys Chem B 113:7170–7177

Birdi KS (2006) Self-assembly monolayer structures of lipids and macromolecules at interfaces. Springer, New York

Boisselier É, Demers É, Cantin L, Salesse C (2017) How to gather useful and valuable information from protein binding measurements using Langmuir lipid monolayers. Adv Colloid Interf Sci 243:60–76

Bouffioux O, Berquand A, Eeman M et al (2007) Molecular organization of surfactin-phospholipid monolayers: effect of phospholipid chain length and polar head. Biochim Biophys Acta Biomembr 1768: 1758–1768

Brockman H (1999) Lipid monolayers: why use half a membrane to characterize protein-membrane interactions? Curr Opin Struct Biol 9:438–443

Chen Y, Vasil AI, Rehaume L et al (2006) Comparison of biophysical and biologic properties of alpha-helical enantiomeric antimicrobial peptides. Chem Biol Drug Des 67:162–173

Clausell A, Busquets MA, Pujol M et al (2004) Polymyxin B-lipid interactions in Langmuir-Blodgett monolayers of Escherichia Coli lipids: a thermodynamic and atomic force microscopy study. Biopolymers 75:480–490

da Silva AVR, De Souza BM, Dos Santos Cabrera MP et al (2014) The effects of the C-terminal amidation of mastoparans on their biological actions and interactions with membrane-mimetic systems. Biochim Biophys Acta 1838:2357–2368

Dathe M, Wieprecht T (1999) Structural features of helical antimicrobial peptides: their potential to modulate activity on model membranes and biological cells. Biochim Biophys Acta Biomembr 1462:71–87

Dennison SR, Harris F, Phoenix DA (2007) The interactions of aurein 1.2 with cancer cell membranes. Biophys Chem 127:78–83

Dennison SR, Morton LHG, Harris F, Phoenix DA (2008) The impact of membrane lipid composition on antimicrobial function of an alpha-helical peptide. Chem Phys Lipids 151:92–102

Dennison SR, Morton LHG, Shorrocks AJ et al (2009) A study on the interactions of Aurein 2.5 with bacterial membranes. Colloids Surf B 68:225–230

Dennison SR, Harris F, Phoenix DA (2010) A Langmuir approach using on monolayer interactions to investigate surface active peptides. Protein Pept Lett 17:1363–1375

Dennison SR, Harris F, Phoenix DA (2014) Langmuir–Blodgett approach to investigate antimicrobial peptide–membrane interactions. Adv Planar Lipid Bilayers Liposomes 20:83–110

Devaux PF (1991) Static and dynamic lipid asymmetry in cell membranes. Biochemistry 30:1163–1173

Devaux PF (1992) Protein involvement in transmembrane lipid asymmetry. Annu Rev Biophys Biomol Struct 21:417–439

Dimova R, Aranda S, Bezlyepkina N et al (2006) A practical guide to giant vesicles. Probing the membrane nanoregime via optical microscopy. J Phys Condens Matter 18:S1151–S1176

Dos Santos Cabrera MP, De Souza BM, Fontana R et al (2004) Conformation and lytic activity of eumenine mastoparan: a new antimicrobial peptide from wasp venom. J Pept Res 64:95–103

Dos Santos Cabrera MP, Alvares DS, Leite NB et al (2011) New insight into the mechanism of action of wasp mastoparan peptides: Lytic activity and clustering observed with giant vesicles. Langmuir 27: 10805–10813

Dos Santos Cabrera MP, Arcisio-Miranda M, Gorjão R et al (2012) Influence of the bilayer composition on the binding and membrane disrupting effect of polybia-MP1, an antimicrobial mastoparan peptide with leukemic T-lymphocyte cell selectivity. Biochemistry 51: 4898–4908

Eeman M, Deleu M (2010) From biological membranes to biomimetic model membranes. Biotechnol Agron Soc Environ 14:719–736

Eeman M, Berquand A, Dufrêne YF et al (2006) Penetration of surfactin into phospholipid monolayers: Nanoscale interfacial organization. Langmuir 22:11337–11345

Epand RM, Vogel HJ (1999) Diversity of antimicrobial peptides and their mechanisms of action. Biochim Biophys Acta Biomembr 1462:11–28

Epand RF, Wang G, Berno B, Epand RM (2009) Lipid segregation explains selective toxicity of a series of fragments derived from the human cathelicidin LL-37. Antimicrob Agents Chemother 53: 3705–3714

Epand RF, Maloy WL, Ramamoorthy A, Epand RM (2010) Probing the "charge cluster mechanism" in amphipathic helical cationic antimicrobial peptides. Biochemistry 49:4076–4084

Fadok VA, Voelker DR, Campbell PA et al (1992) Exposure of phosphatidylserine on the surface of apoptotic lymphocytes triggers specific recognition and removal by macrophages. J Immunol 148: 2207–2216

Fadok VA, Bratton DL, Frasch SC et al (1998) The role of phosphatidylserine in recognition of apoptotic cells by phagocytes. Cell Death Differ 5:551–562

Fidelio GD, Maggio B, Cumar FA (1986) Interaction of melittin with glycosphingolipids and phospholipids in mixed monolayers at different temperatures. Effect of the lipid physical state. Biochim Biophys Acta Biomembr 862:49–56

Fischer A, Lösche M, Möhwald H, Sackmann E (1984) On the nature of the lipid monolayer phase transition. J Phys Lett 45:785–791

Fjell CD, Hiss JA, Hancock REW, Schneider G (2012) Designing antimicrobial peptides: form follows function. Nat Rev Drug Discov 11: 37–51

Fošnarič M, Iglič A, May S (2006) Influence of rigid inclusions on the bending elasticity of a lipid membrane. Phys Rev E 74:1–12

Grimsley GR, Scholtz JM, Pace CN (2009) A summary of the measured pK values of the ionizable groups in folded proteins. Protein Sci 18: 247–251

Hädicke A, Blume A (2016) Binding of the cationic peptide (KL)4K to lipid Monolayers at the air–water Interface: effect of lipid Headgroup charge, Acyl chain length, and Acyl chain saturation. J Phys Chem B 120:3880–3887

Hancock RE, Falla T, Brown M (1995) Cationic bactericidal peptides. Adv Microb Physiol 37:135–175

Haney EF, Nathoo S, Vogel HJ, Prenner EJ (2010) Induction of non-lamellar lipid phases by antimicrobial peptides: a potential link to mode of action. Chem Phys Lipids 163:82–93

He K, Ludtke SJ, Huang HW, Worcester DL (1995) Antimicrobial peptide pores in membranes detected by neutron in-plane scattering. Biochemistry 34:15614–15618

Heckl WM, Losche M, Cadenhead DA, Mohwald H (1986) Electrostatically induced growth of spiral lipid domains in the presence of cholesterol. Eur Biophys J Biophys Lett 14:11–17

Henon S, Meunier J (1991) Microscope at the Brewster angle: direct observation of first-order phase transitions in monolayer. Rev Sci Instrum 62:936–939

Hoenig D, Moebius D (1991) Direct visualization of monolayers at the air-water interface by Brewster angle microscopy. J Phys Chem 95: 4590–4592

Hope MJ, Bally MB, Webb G, Cullis PR (1985) Production of large unilamellar vesicles by a rapid extrusion procedure. Characterization of size distribution, trapped volume and ability to maintain a membrane potential. Biochim Biophys Acta Biomembr 812:55–65

Hope MJ, Bally MB, Mayer LD et al (1986) Generation of multilamellar and unilamellar phospholipid vesicles. Chem Phys Lipids 40:89–107

Huang HW, Chen FY, Lee MT (2004) Molecular mechanism of peptide-induced pores in membranes. Phys Rev Lett 92:198304–198301

Ishii H, Mori T, Shiratsuchi A et al (2005) Distinct localization of lipid rafts and externalized phosphatidylserine at the surface of apoptotic cells. Biochem Biophys Res Commun 327:94–99

Islam MZ, Alam JM, Tamba Y et al (2014) The single GUV method for revealing the functions of antimicrobial, pore-forming toxin, and cell-penetrating peptides or proteins. Phys Chem Chem Phys 16: 15752–15767

Jin Y, Hammer J, Pate M et al (2005) Antimicrobial activities and structures of two linear cationic peptide families with various amphipathic β-sheet and α-helical potentials. Antimicrob Agents Chemother 49:4957–4964

Jing W, Hunter HN, Hagel J, Vogel HJ (2003) The structure of the antimicrobial peptide ac-RRWWRF-NH2 bound to micelles and its interactions with phospholipid bilayers. J Pept Res 61:219–229

Kaganer V, Möhwald H, Dutta P (1999) Structure and phase transitions in Langmuir monolayers. Rev Mod Phys 71:779–819

Klocek G, Schulthess T, Shai Y, Seelig J (2009) Thermodynamics of melittin binding to lipid bilayers. Aggregation and pore formation. Biochemistry 48:2586–2596

Ladokhin AS, Wimley WC, White SH (1995) Leakage of membrane vesicle contents: determination of mechanism using fluorescence requenching. Biophys J 69:1964–1971

Leite NB, Da Costa LC, Alvares DS et al (2011) The effect of acidic residues and amphipathicity on the lytic activities of mastoparan peptides studied by fluorescence and CD spectroscopy. Amino Acids 40:91–100

Leite NB, Aufderhorst-Roberts A, Palma MS et al (2015) PE and PS lipids synergistically enhance membrane Poration by a peptide with anticancer properties. Biophys J 109:936–947

Lheveder C, Hénon S, Meunier J (2000) Brewster angle microscopy. In: Baszkin A, Norde W (eds) Physical chemistry of biological interfaces. Marcel Dekker, New York, p 848

Lösche M, Sackmann E, Möhwald H (1983) A fluorescence microscopic study concerning the phase diagram of phospholipids. Ber Bunsenges Phys Chem 87:848–852

Maget-Dana R (1999) The monolayer technique: a potent tool for studying the interfacial properties of antimicrobial and membrane-lytic peptides and their interactions with lipid membranes. Biochim Biophys Acta Biomembr 1462:109–140

Maget-Dana R, Lelièvre D, Brack A (1999) Surface active properties of amphiphilic sequential isopeptides: comparison between α-helical and β-sheet conformations. Biopolymers 49:415–423

Malanovic N, Lohner K (2015) Gram-positive bacterial cell envelopes: the impact on the activity of antimicrobial peptides. Biochim Biophys Acta 1858:936–946

Maltseva E, Shapovalov VL, Möhwald H, Brezesinski G (2006) Ionization state and structure of L-1,2-dipalmitoylphosphatidylglycerol monolayers at the liquid/air interface. J Phys Chem B 110:919–926

Mangiarotti A, Wilke N (2015) Energetics of the phase transition in free-standing versus supported lipid membranes. J Phys Chem B 119: 8718–8724

Marassi FM, Opella SJ (2000) A solid-state NMR index of helical membrane protein structure and topology. J Magn Reson 144:150–155

Marsh D (1996) Lateral pressure in membranes. Biochim Biophys Acta Rev Biomembr 1286:183–223

Marshall SH, Arenas G (2003) Antimicrobial peptides: a natural alternative to chemical antibiotics and a potential for applied biotechnology. Electron J Biotechnol 6:271–284

Matsuzaki K, Murase O, Fujii N, Miyajima K (1996a) An antimicrobial peptide, magainin 2, induced rapid flip-flop of phospholipids coupled with pore formation and peptide translocation. Biochemistry 35:11361–11368

Matsuzaki K, Yoneyama S, Murase O, Miyajima K (1996b) Transbilayer transport of ions and lipids coupled with mastoparan X translocation. Biochemistry 35:8450–8456

May S, Harries D, Ben-shaul A (2000) Lipid Demixing and protein-protein interactions in the adsorption of charged proteins on mixed membranes. Biophys J 79:1747–1760

McConlogue CW, Vanderlick TK (1997) A close look at domain formation in DPPC Monolayers. Langmuir 13:7158–7164

McElhaney RN (1982) The use of differential scanning calorimetry and differential thermal analysis in studies of model and biological membranes. Chem Phys Lipids 30:229–259

McElhaney RN (1986) Differential scanning calorimetric studies of lipid-protein interactions in model membrane systems. Biochim Biophys Acta 864:361–421

Miller A, Mohwald H (1987) Diffusion limited growth of crystalline domains in phospholipid monolayers. J Chem Phys 86:4258–4265

Mohwald H (1990) Phospholipid and Phospholipid-protein Monolayers at the air/water Interface. Annu Rev Phys Chem 41:441–476

Möhwald H (1995) Phospholipid monolayers. In: Lipowsky R, Sackmann E (eds) Handbook of biological physics, vol 1. Elsevier, Netherlands, pp 161–211

Mottola M, Wilke N, Benedini L et al (2013) Ascorbyl palmitate interaction with phospholipid monolayers: electrostatic and rheological preponderancy. Biochim Biophys Acta Biomembr 1828:2496–2505

Mularski A, Wilksch JJ, Wang H et al (2015) Atomic force microscopy reveals the Mechanobiology of Lytic peptide action on bacteria. Langmuir 31:6164–6171

Mura M, Dennison SR, Zvelindovsky AV, Phoenix DA (2013) Aurein 2.3 functionality is supported by oblique orientated alpha-helical formation. Biochim Biophys Acta Biomembr 1828:586–594

Neville F, Cahuzac M, Konovalov O et al (2006) Lipid headgroup discrimination by antimicrobial peptide LL-37: insight into mechanism of action. Biophys J 90:1275–1287

Nguyen LT, Haney EF, Vogel HJ (2011) The expanding scope of antimicrobial peptide structures and their modes of action. Trends Biotechnol 29:464–472

O'Neill J (2015) Tackling a global health crisis: initial steps The Review on Antimicrobial Resistance Chaired The Review on Antimicrobial Resistance, Chaired by Jim O'Neill

Parente RA, Nir S, Szoka FC (1990) Mechanism of leakage of phospholipid vesicle contents induced by the peptide GALA. Biochemistry 29:8720–8728

Patel H, Tscheka C, Heerklotz H (2009) Characterizing vesicle leakage by fluorescence lifetime measurements. Soft Matter 5:2849

Pokorny A, Birkbeck TH, Almeida PFF (2002) Mechanism and kinetics of δ-lysin interaction with phospholipid vesicles. Biochemistry 41: 11044–11056

Puff N, Angelova MI (2006) Lipid vesicles-development and applications for studding membrane heterogeneity and interactions. Adv Planar Lipid Bilayer Liposomes 5:173–228

Quinn PJ (2010) A lipid matrix model of membrane raft structure. Prog Lipid Res 49:390–406

Rautenbach M, Gerstner GD, Vlok NM et al (2006) Analyses of dose–response curves to compare the antimicrobial activity of model cationic α-helical peptides highlights the necessity for a minimum of two activity parameters. Anal Biochem 350:81–90

Riske KA (2015) Optical microscopy of giant vesicles as a tool to reveal the mechanism of action of antimicrobial peptides and the specific case of Gomesin. Adv Planar Lipid Bilayer Liposomes 21:99–129

Rosetti CM, Mangiarotti A, Wilke N (2017) Sizes of lipid domains: what do we know from artificial lipid membranes? What are the possible shared features with membrane rafts in cells? Biochim Biophys Acta Biomembr 1859:789–802

Rothman JE, Lenard J (1977) Membrane asymmetry. Science 195:743–753

Seelig A (1990) Substance P and antagonists. Surface activity and molecular shapes. Biochim Biophys Acta Biomembr 1030: 111–118

Sengupta D, Leontiadou H, Mark AE, Marrink SJ (2008) Toroidal pores formed by antimicrobial peptides show significant disorder. Biochim Biophys Acta Biomembr 1778:2308–2317

Sezgin E, Levental I, Mayor S, Eggeling C (2017) The mystery of membrane organization: composition, regulation and roles of lipid rafts. Nat Rev Mol Cell Biol 18:361–374

Sforça ML, Oyama S, Canduri F et al (2004) How C-terminal carboxyamidation alters the biological activity of peptides from the venom of the eumenine solitary wasp. Biochemistry 43:5608–5617

Shai Y (1999) Mechanism of the binding, insertion and destabilization of phospholipid bilayer membranes by alpha-helical antimicrobial and cell non-selective membrane-lytic peptides. Biochim Biophys Acta Biomembr 1462:55–70

Silvestro L, Axelsen PH (2000) Membrane-induced folding of Cecropin A. Biophys J 79:1465–1477

Spaar A, Münster C, Salditt T (2004) Conformation of peptides in lipid membranes studied by x-ray grazing incidence scattering. Biophys J 87:396–407

Stafford JH, Thorpe PE (2011) Increased exposure of phosphatidylethanolamine on the surface of tumor vascular endothelium. Neoplasia 13:299–308

Stefaniu C, Brezesinski G, Möhwald H (2014) Langmuir monolayers as models to study processes at membrane surfaces. Adv Colloid Interf Sci 208:197–213

Tamba Y, Terashima H, Yamazaki M (2011) A membrane filtering method for the purification of giant unilamellar vesicles. Chem Phys Lipids 164:351–358

Travkova OG, Brezesinski G (2013) Adsorption of the antimicrobial peptide arenicin and its linear derivative to model membranes - a maximum insertion pressure study. Chem Phys Lipids 167–168:43–50

Utsugi T, Schroit AJ, Connor J et al (1991) Elevated expression of phosphatidylserine in the outer membrane leaflet of human tumor cells and recognition by activated human blood monocytes. Cancer Res 51:3062–3066

Vanderlick TK, Möhwald H (1990) Mode selection and shape transition of phospholipid monolayer domains. J Phys Chem 94:886–890

Vega Mercado F, Maggio B, Wilke N (2011) Phase diagram of mixed monolayers of stearic acid and dimyristoylphosphatidylcholine. Effect of the acid ionization. Chem Phys Lipids 164:386–392

Vega Mercado F, Maggio B, Wilke N (2012) Modulation of the domain topography of biphasic monolayers of stearic acid and dimyristoyl phosphatidylcholine. Chem Phys Lipids 165:232–237

Wade D, Boman A, Wåhlin B et al (1990) All-D amino acid-containing channel-forming antibiotic peptides. Proc Natl Acad Sci U S A 87: 4761–4765

Wang G (2014) Human antimicrobial peptides and proteins. Pharmaceuticals (Basel) 7:545–594

Wang K, Zhang B, Zhang W et al (2008) Antitumor effects, cell selectivity and structure-activity relationship of a novel antimicrobial peptide polybia-MPI. Peptides 29:963–968

Wang K, Yan J, Zhang B et al (2009) Novel mode of action of polybia-MPI, a novel antimicrobial peptide, in multi-drug resistant leukemic cells. Cancer Lett 278:65–72

Wang K, Yan J, Chen R et al (2012) Membrane-active action mode of polybia-CP, a novel antimicrobial peptide isolated from the venom of Polybia paulista. Antimicrob Agents Chemother 56: 3318–3323

Weinberger A, Tsai F-C, Koenderink GH et al (2013) Gel-assisted formation of Giant Unilamellar vesicles. Biophys J 105:154–164

Weis RM, McConnell HM (1984) Two-dimensional chiral crystals of phospholipid. Nature 310:47–49

Wilke N (2014) Lipid monolayers at the air-water interface: a tool for understanding electrostatic interactions and rheology in biomembranes. Adv Planar Lipid Bilayer Liposomes 20:51–81

Wimley WC (2010) Describing the mechanism of antimicrobial peptide action with the interfacial activity model. ACS Chem Biol 5:905–917

Wimley WC, Hristova K (2011) Antimicrobial peptides: successes, challenges and unanswered questions. J Membr Biol 239:27–34

Worthman LA, Nag K, Davis PJ, Keough KM (1997) Cholesterol in condensed and fluid phosphatidylcholine monolayers studied by epifluorescence microscopy. Biophys J 72:2569–2580

Yamazaki M, Tamba Y (2005) The single GUV method for probing biomembrane structure and function. e-J Surf Sci Nanotechnol 3: 218–227

Yandek LE, Pokorny A, Almeida PFF (2009) Wasp mastoparans follow the same mechanism as the cell-penetrating peptide transportan 10. Biochemistry 48:7342–7351

Yeaman MR, Yount NY (2003) Mechanisms of antimicrobial peptide action and resistance. Pharmacol Rev 55:27–55

Yeung ATY, Gellatly SL, Hancock REW (2011) Multifunctional cationic host defence peptides and their clinical applications. Cell Mol Life Sci 68:2161–2176

Zanin LMP, Alvares DS, Juliano MA et al (2013) Interaction of a synthetic antimicrobial peptide with model membrane by fluorescence spectroscopy. Eur Biophys J 42:819–831

Zanin LPM, de Araujo AS, Juliano MA et al (2016) Effects of N-terminus modifications on the conformation and permeation activities of the synthetic peptide L1A. Amino Acids 48:1433–1444

Zasloff M (2002) Antimicrobial peptides of multicellular organisms. Nature 415:389–395

Zemel A, Ben-Shaul A, May S (2008) Modulation of the spontaneous curvature and bending rigidity of lipid membranes by interfacially adsorbed amphipathic peptides. J Phys Chem B 112:6988–6996